

**Arno Ylitalo**

**Clever-1 in cancer – Assessing the efficacy of a novel immunotherapy approach in patient derived explant cultures**

**Syventävien opintojen kirjallinen työ**

**Kevätlukukausi 2020**

**Arno Ylitalo**

**Clever-1 in cancer – Assessing the efficacy of a novel immunotherapy approach in patient derived explant cultures**

**Biolääketieteen laitos, Turun yliopisto**

**MediCity laboratories, Hollmén group, Biocity**

**Kevätlukukausi 2020**

**Ohjaaja: Dosentti Maija Hollmén**

**Lähiohjaaja: FT Reetta Virtakoivu**

*The originality of this thesis has been checked in accordance with the University of Turku quality assurance system using the Turnitin OriginalityCheck service.*

YLITALO, ARNO: Clever-1 in cancer – Assessing the efficacy of a novel immunotherapy approach in patient derived explant cultures

Syventävien opintojen kirjallinen työ, 23s  
Syöpä, infektiot ja immuniteetti  
Tammikuu 2020

---

Onkologisten hoitojen tehokkuus on kehittynyt paljon viimeisten vuosikymmenten aikana, mutta lukuisille syöpätyypeille ei edelleenkään ole tehokasta hoitoa. Syövän immuunihoidoissa ohjataan potilaan omaa immuunijärjestelmää tuhoamaan syöpäsolut. Näin voidaan osittain välttää tai vähentää toksisten sytostaattihoidojen käyttöä onkologiassa. Immuunihoidoilla yksin tai yhdistämällä ne perinteisiin syöpähoitoihin on saatu ennennäkemättömiä tuloksia syövän ja sen metastaasien reduktiossa. Eräs aktiivisen immuuniterapian muoto on ICB-hoito (immune checkpoint blockade), jossa elimistön immuunijärjestelmän syöpää vastustavat ominaisuudet pyritään aktivoimaan. Tähän perustuva, immunosuppressiivisiin makrofageihin vaikuttava anti-Clever-1 vasta-aine on uusi mahdollinen immuno-onkologinen hoito. Clever-1 vasta-ainetta on jo käytetty vaiheen I/II kliinisissä kokeissa syöpäpotilailla. Tässä tutkimuksessa selvitettiin Clever-1 vasta-ainehoidon biologisia vaikutuksia ihmisen syöpäkudoksessa ex vivo.

Turun yliopistollisesta keskussairaalaasta saatujen rintasyöpänäytteiden avulla pystyimme tutkimaan Clever-1 positiivisten makrofagien ja T-solujen määrää kasvainkudoksessa ja niiden sijoittumista kasvaimen mikroympäristössä käyttäen immunohistokemiallisia menetelmiä. Lisäksi, teimme kokeen, missä käsitelimme potilaiden kasvainkudosta vastaavien potilaiden verestä eristetyillä perifeerisillä mononukleaarisilla soluilla (PBMC, peripheral blood mononuclear cell), joita oli käsitelty anti-Clever-1 vasta-aineella. Tässä tutkimme käsiteltyjen solujen vaikutusta syöpäsoluihin ja kasvainkudoksessa indusoituneen apoptoosin määrää kvalitatiivisesti.

Tämä ainutlaatuinen koe mahdollisti kasvainkudoksen biologisen vasteen kuvantamista paremmin kuin aiemmin yleisesti käytetyllä kaksisolotteisella solukasvatuksella. Koe osoitti, kuinka potilaan käsitellyt PBMC solut infiltroivat kasvainkudokseen ja aiheuttavat apoptoosia kasvainkudoksessa, kun soluja esikäsiteltiin anti-Clever-1 vasta-aineella.

Avainsanat: ICB-hoito, immuno-onkologia, vasta-aine, M2-makrofagit

# Contents

|  |    |
|--|----|
| 1. Introduction  | 2  |
| 2. Review of the literature  | 3  |
| 2.1 Cancer and the immune system   | 3  |
| 2.2 How tumors evade the immune system   | 4  |
| 2.3 Cell composition in the tumor microenvironment                                     | 5  |
| 2.4 Immune checkpoint targeting  | 7  |
| 2.5 Clever-1 in cancer   | 8  |
| 3. Materials and methods   | 9  |
| 3.1 Tissue samples   | 9  |
| 3.2 Tumor ex vivo explant assay with stained PBMCs                                     | 10 |
| 3.2.1 PBMC treatment   | 10 |
| 3.2.2 Tumor sample coculture with PBMCs  | 10 |
| 3.3 Immunohistochemistry   | 11 |
| 3.4 Imaging  | 11 |
| 3.5 Statistical methods  | 12 |
| 4. Results   | 12 |
| 4.1 The tissue structure and cell composition changes in mammary gland adenocarcinoma  | 12 |
| 4.2 Clever-1+ macrophages and CD8+ T cells are expressed in the tumor microenvironment | 13 |
| 4.3 IHC staining cell counts   | 14 |
| 4.4 Treated PBMCs migrate into the tumor tissue  | 16 |
| 4.5 Anti-Clever-1 antibody treated leukocytes induce apoptosis in tumor cells          | 16 |
| 5. Discussion  | 20 |
| 6. References  | 23 |

# 1. Introduction

Cancer is a disease with variety of recognized forms and remains the most significant cause of death in most parts of the world with 9.6 million deaths annually (1). The complexity and plasticity of cancer makes it the most studied disease in medicine. In modern clinical use there are a plenty of treatments for cancer, many of them still with poor curative treatment. Even though cancer is expressed in many forms, the same essential hallmarks of development can be recognized in all types of neoplastic disease. Learning the biological foundation to these hallmarks of cancer and developing combinatory therapies, are the key to eventually curing cancer.

In the pathogenesis of neoplastic disease, increased attention in research is given to the “tumor microenvironment” and its function on tumor development. Immunotherapies target the cells that interplay in the tumorigenesis and activate the patient’s own immune system in the fight against cancer. The immune cell composition of the tumor has shown to be a good prognostic marker for the outcome of the disease. While the immune system is responsible for the depletion of cancer cells, there are known to be immune cells with pro-tumor effect and anti-inflammatory properties when interacting with cancer cells. Relatively new area of cancer treatment, called immune checkpoint blockade (ICB) therapies, targets the key regulators of the immune system and induce inflammatory activation, aiming to re-establish inflammation in the site of the tumor. However, the success of this immunotherapy varies in patients and the treatment’s biological basis still remains unknown in many ways.

In this study we concentrate on particular immunosuppressive cells called M2-type macrophages and tumor associated macrophages (TAMs). These macrophages are known to express Clever-1, Common Lymphatic Endothelial and Vascular Endothelial Receptor 1, which has been shown to play a major role in inducing the anti-inflammatory phenotype of these macrophages in many types of cancer. The effect of anti-Clever-1 antibody blockade in converting these M2-macrophages was evaluated. Also, peripheral blood monocytes into anti-tumor or M1-type macrophages that activate the immune cells like effector T-cells and eventually cause apoptosis and reduction of cancer cells was studied. Humanized anti-Clever-1 antibody is already in phase I/II clinical trials in cancer patients with selected metastatic or inoperable solid tumors and this study is aimed to help to understand the biological effect of this drug in cancer.

## 2. Review of the literature

### 2.1 Cancer and the immune system

The immune system is a highly developed biological factor in all mammals, attributing in defence against noxious microbes and in managing inflammatory response. The immune system is also essential in detecting the body's own damaged or mutated cells. The immune system consists of variety of cells mostly proliferated from multipotential hematopoietic stem cells in the bone marrow. Dividing to myeloid and lymphoid cells, an effective immune system is formed with the use of lymph structures and vasculature. How well the immune system is able to counteract tumor development is relevant to cancer prognosis.

Innate and adaptive parts of the immune system are essential in preventing early tumor development and destroying cells with oncogenic properties. A study conducted by Teng and colleagues demonstrated (2), that mice with insufficient T and NK cell types show higher incidence of tumor development in comparison to wild type mice. In the early phase of tumor development, inflammation is present and cancer cell are destroyed effectively by the coordinated immune cells (Figure 1).

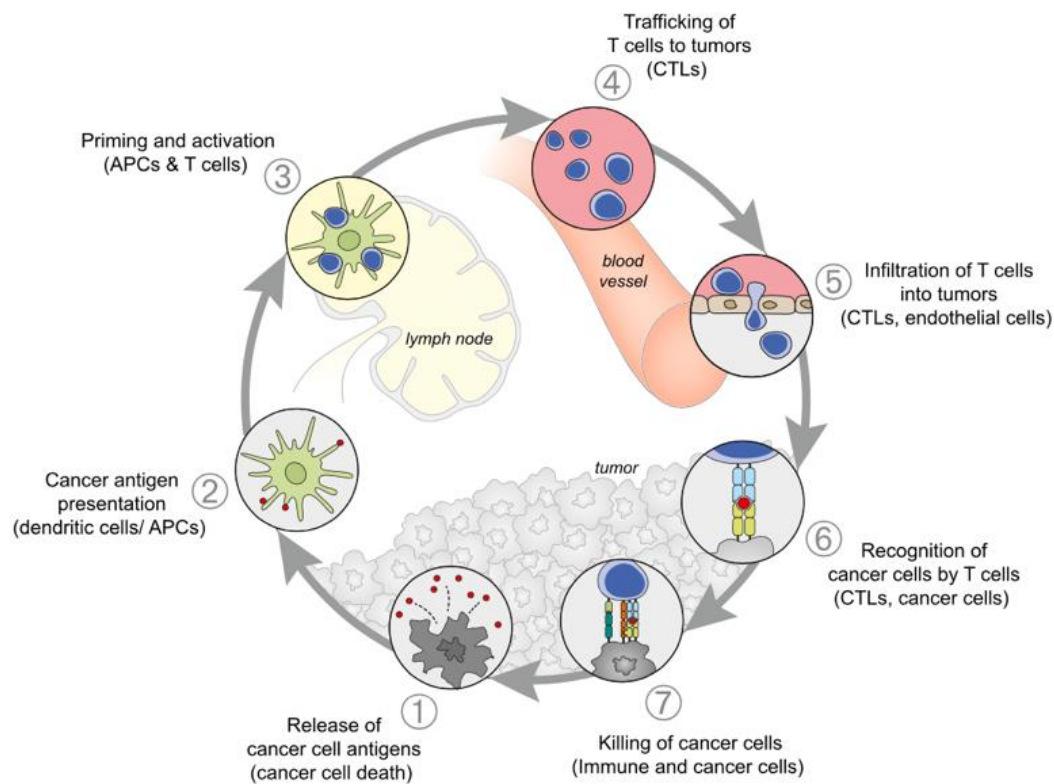


Figure 1: How the immune system counteracts early tumor development. APCs = antigen presenting cells. CTLs = cytotoxic T lymphocytes. Source: Immunity 2013; 39(1) 1-10

On the other hand, cancer has been shown to be associated with other types of inflammation that are not aroused by tumors. Low-grade inflammation caused by diet or substances like tobacco is shown to have direct correlation to elevated risk for developing various cancers (3). In contradiction, inducing local acute inflammation by introduction of *Mycobacterium bovis* bacteria to the cancer site has been shown to successfully treat squamous cell carcinoma of the bladder (4). This emphasizes the fact that the effect of the immune system to cancer and vice versa, is not straight forward and comprises of a multitude of different factors.

## 2.2 How tumors evade the immune system

Cancer cells being by definition epigenetically and genetically unstable, with the accumulation of random mutations, they end up developing many ways to hide from the immune system and misguide the immune cells to work pro-tumor instead. Cancer growth and metastasis would not be possible without the inhibition of inflammation and reduced activation of anti-tumor effect of the immune system. In early tumor development phase, the immune system recognizes cancer cells by their characteristic cell surface complexes. Downregulation of MHC I/II antigens on malignant tumor cells in metastatic melanoma was addressed by S. Rodig and colleagues (6). Downregulation of the tumor antigens or so called neoantigens, leads to decreased activation of dendritic cells (DCs) resulting in promoted tumor growth (figure 2A).

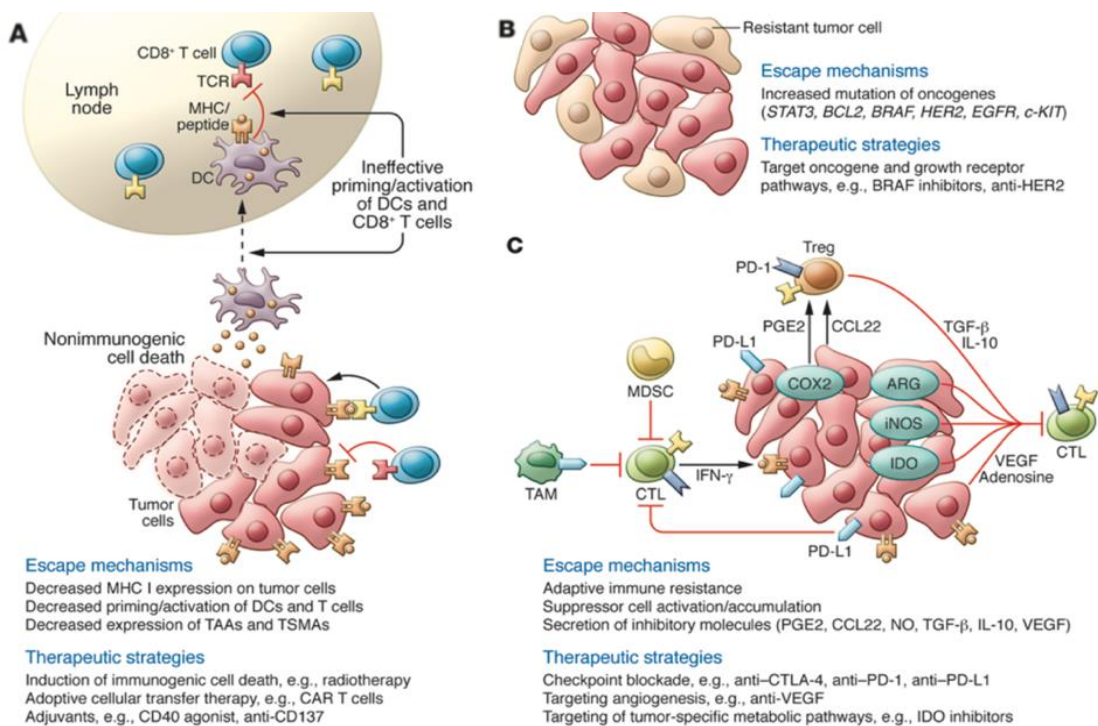


Figure 2: The ways on how the cancer cells evade the immune system Source: J Clin Invest 2015; 125(9): 3338-46

Moreover, cancer cells can have upregulated mechanisms to survive against cytotoxic properties of the immune system. It is common for cancer cells to multiply the transcription of growth or survival agonist genes. For example, the overexpression of the gene that codes human epidermal growth factor receptor 2 (HER2) appears in approximately 20% of breast cancer patients with aggressive clinical phenotype (5). Some therapeutic strategies for cancer, target specifically these growth factor pathways (figure 2B) through antibody and inhibitory molecules, but are phased with the problem of pathologically mutating cancer cells.

In addition, and most importantly related to the present study, are the means of immunosuppression in TME (figure 2C). Cancer cells secrete a variance of different inhibitory cytokines such as IL-10, lactate and transforming growth factor beta 1 (TGF $\beta$ 1) that produce systematic immunosuppression (7-9). What is more, cancer cells appear to produce immunosuppression by activating immune checkpoint receptors such as CTLA-4 and PD-1 on T cells (10) or Clever-1 on macrophages (11).

### 2.3 Cell composition in the tumor microenvironment

Tumors are always unique with their own biological properties varying even in tumors proliferated from the same parts of the tissue. In cancer immunology, an essential term in research is the tumor microenvironment (TME). The TME describes the important cellular properties surrounding the tumor including the connective tissue and the extracellular matrix and all the associated immune cells. All the cells in the TME effect tumor behavior with constant contact and interaction with each other. Correlation studies of certain cell compositions of different tumors in relation to life expectancy prognosis, has led to assumptions on the significance of certain cells in cancer. Recognizing the important hallmarks in the TME, especially it's immune cell composition, is essential in developing effective personalized cancer immunotherapy.

Natural killer cells (NK) are innate immune cells circulating in the entire vascular system. They activate when in contact with infected or malignant cells. NK cells express a large scale of receptors that are used in immune surveillance. The NK cell activation is not dependent of neoantigen detection, also in the absence of MHC proteins on cancer cell membranes, NK cells produce cytokines like IFN- $\gamma$  and thus marks cancer cells for programmed cell death (6). There are no shown pro-tumor aspects of NK cells, but there are solid conclusions that they can have a large impact as a part of the TME and they work in suppressing tumor growth as demonstrated by Iannello and colleagues in 2016 (12).

Granulocytes are myeloid derived cells that play a large role in producing inflammatory response in the body. They're divided to mast cells, eosinophils, basophils and neutrophils. These cells are known to be important in a fast response to pathogens and inflammation related to tissue modulation and repair.



It has been suspected that granulocytes also function in the TME with pro-tumor properties secreting immunosuppressive chemokines (13) and in inducing angiogenesis and lymphangiogenesis (14). High consistency of neutrophils in the TME, but also the patients' blood/lymphocyte ratio, has been shown to correlate with adverse prognosis in various cancers (15).

Other myeloid tissue derived cells are dendritic cells and macrophages. As reviewed in chapter 2.2, the absence of MHC proteins, which are the most important neoantigens in dendritic cell activation, results in decreased CD8<sup>+</sup> T cell and NK cell activation and promotes the tumor growth. Thus, dendritic cells work as mediators in adaptive immunity as antigen-presenting cells (APCs), but their mechanism in tumor progression, remains understudied. Macrophages have proven to be a promising approach in immunologic treatments for cancer and are the most abundant form of immune cells found in the TME. Macrophages differentiate from circulating monocytes after penetrating into tissues. In addition, a different type of macrophages called yolk-sac derived tissue-resident macrophages are present in tissues. Macrophages are very polymorphic in their ability to transform their phenotype according to their homeostatic activity (16). High density of tumor associated macrophages (TAMs) and also the expression of macrophage specific markers correlates with a poor prognosis in the meta-analysis authored by Zhang et al. 2012 (17). In the contrary the same meta-analysis displayed positive prognosis in patients with prostate, lung, stomach bone malignancies expressing the macrophage specific markers. This data has led to the division of two subsets of macrophages: the inflammation inducing M1-type macrophages and M2-type with pro-tumor and immunosuppressive properties. Manipulating the phenotype of these TAMs has proved promising results in generating anti-tumor inflammation. With the blockage of Clever-1 receptor that manifests on M2-type macrophages, the macrophages seem to turn from immunosuppressive to pro-inflammatory and activate CD8<sup>+</sup> T cells in the TME and reduce tumor growth significantly (11).

Lymphocytes, the key components of adaptive immune system, can be divided into two categories: B cells and T cells. The emergence of B cells in the TME has been shown in pancreatic and also gastric carcinomas recently by Murakami Y et al. 2019 (18), showing elements of B cells with pro-tumor properties. T cells have also been the main focus on immune-oncological research since the promising results, in the late 90s, showing that blocking of T cell inhibitory signals, such as the cytotoxic T-lymphocyte-associated protein 4 (CTLA-4) receptor, enhance anti-tumor response in immunosuppressive tumors. T cells migrate to the TME in early phase of tumor development and suppress the growth of immunogenic cancer cells. CD4<sup>+</sup> T cells or "helper" T cells secrete cytokines such as IL-2 and TNF- $\alpha$  that activate inflammation by effecting macrophages and NK cells and also CD8<sup>+</sup> T cells or "effector" T-cells. Upon activation, CD8<sup>+</sup> T cells differentiate into cytotoxic T

lymphocytes (CTLs). In close contact with cancer cells, CTLs secrete anti-tumor cytokines through exocytosis which effectively destroy their target cells as described in the study conducted by *Matsushita* and colleagues in 2012 (19). It is the inhibitory signals that arise in the TME that impact the tumor reducing function of the T cells.

## 2.4 Immune checkpoint targeting

The advances in molecular immunology has shed light upon the complexity of all the microlevel mechanisms that influence the definite immune response. Immune checkpoint blockade (ICB) therapy effects these modulating aspects of the innate and adaptive immune system and harness the full potential of the individuals own immune system in reducing disease duration and development. Many modern cancer treatments require an inflamed tumor site, which is only present in few advanced phase cancers. ICB therapies open the tumor site for many treatments by re-engaging inflammation. The specificity of the action of T cells is astounding since they have the ability to produce as many as  $10^{15}$  different antigen receptors on their cell surface (20) and thus the immune system has the potential to match the complexity and adaptability of cancer.

The first immune checkpoint targeting antibody to proceeded into clinical trials was CTLA-4 receptor targeting, fully human antibody, ipilimumab (Medarex, Bristol-Myers Squibb). CTLA-4 receptor is found on the cell surface of T-cells and produces, when active, an inhibitory signal for the cytotoxic function of the cell. Blocking this receptor with an anti-CTLA-4 antibody (ipilimumab) resulted in promising clinical response in phase III trials where patients with advanced melanoma were treated with ipilimumab. Immediate improvement in survival rates was seen (21) and in addition, a long-term follow-up review indicated a 20% increase in 4-year survival rate. Moreover, this treatment proved to be very effective suggesting a survival of 10 years or more for some of the patients (22). Ipilimumab was the first FDA-accepted ICB-therapy for clinical use in 2011.

This followed numerous studies investigating these immunosuppressive pathways in immune cells and antibodies targeting the T-cell associated programmed cell death protein (PD-1) and its ligand PD-L1 (Figure 3), which have also shown much promise in clinical trials and are often used in combination with the anti-CTLA-4 treatment (6). On the other hand, there are some adverse effects related to these therapies. By creating an unbalance to the immune system, immunotherapies have shown to produce various toxic effects (23). As an another addition to the many side-effects already treated in oncology, the treatment of these side effects with steroids also result in greater immunosuppression and diminished drug effect.

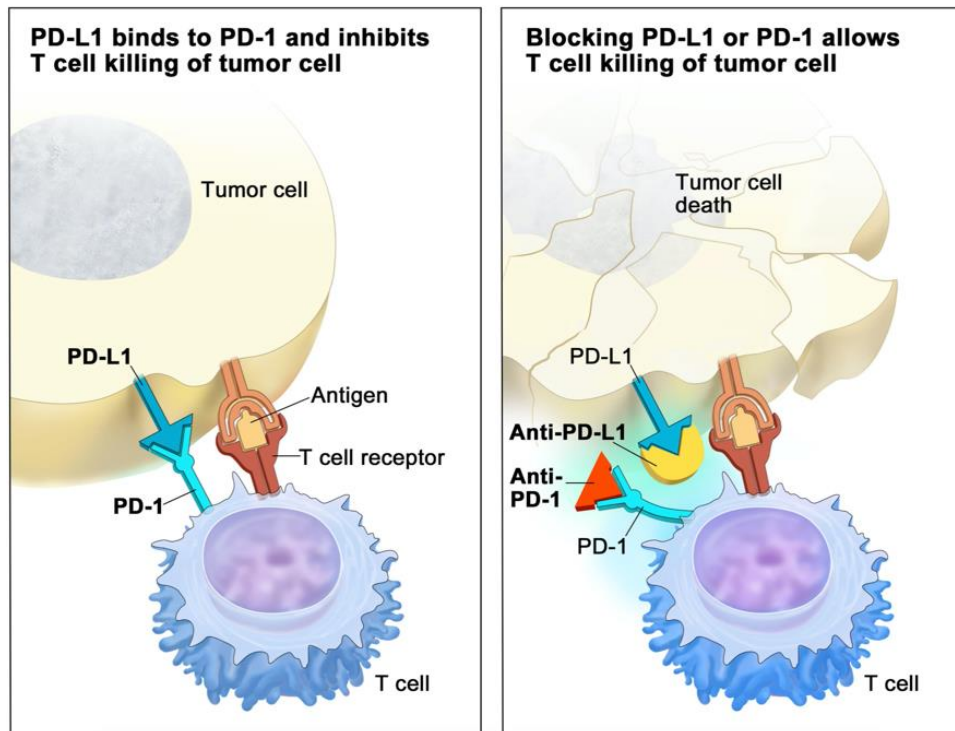


Figure 3: The biological basis of anti-PD-1 and anti-PD-L1 therapies. <https://www.cancer.gov>

Since cancer immunotherapies target the immune cells instead of the cancer cells, these treatments have applications in various types of cancer that have mutated and developed in histologically different sites in the body. Secondly, the blockade of these immune checkpoints in the TME results in higher inflammation in the tumor site where, before treatment, there was no longer an active inflammation. Many tumors develop such high immunosuppression that all forms of active inflammation are diminished and many effective cancer therapies rely on this. Targeting the immune checkpoints in immune cells thus opens a possibility to use ICB therapies alongside with classic forms of cancer treatment.

## 2.5 Clever-1 in cancer

Successful cancer immunotherapy requires an activated antitumor immune cell activation, most importantly by the adaptive immune system and CD8<sup>+</sup> T cell population in the TME. In most advanced malignant cancers, the tumors are noninflammatory, thus resilient of immunotherapy. Solution to this has been researched in manipulating the immunosuppressive mechanisms in the TME. Particularly the most prominent immune cell in the TME, TAMs have shown to predict bad prognosis in many types of cancers (16). Targeting these macrophages has potential in increasing combinatory effect of cytoreductive therapies (chemotherapy and radiotherapy) and immunotherapeutic approaches (24).

Common lymphatic endothelial and vascular endothelial receptor-1 or Clever-1 (also known as Stabilin-1 or FEEL-1) is coded by the Stab-1 gene. It is a transmembrane receptor with a multitude of properties and is highly expressed in endothelial cells and M2- type macrophages (24). On endothelial cells Clever-1 is associated with leukocyte infiltration to the site of inflammation and is also expressed in various angiogenic conditions. Clever-1 functions in macrophages as a scavenger receptor participating in endocytosis and recycling of cellular materials (25). A study conducted by Palani and colleagues in 2016 (26) found that Clever-1 is also expressed in peripheral blood monocytes. In addition, a suppressive effect of Clever-1 positive monocytes on CD4+ “helper” T -cells was shown.

As addressed in chapter 2.3, M2- type macrophages induce immunosuppression and facilitate tumor growth. Clever-1 is known to be associated with the M2-type macrophages and TAMs since Clever-1 knockout mice as well as anti-Clever-1 treated mice showed lower quantities of these macrophages in tumor sites (26). Moreover, Viitala and colleagues showed that macrophages not expressing Clever-1 correlated with a more immunostimulatory phenotype. What is more, the anti-tumor activation of CD8+ T cells was achieved when Clever-1 was blocked with an anti-Clever-1 antibody (11).

The aim of this study was to investigate the role of Clever-1 positive monocytes and macrophages in breast cancer and to study how the inhibition of Clever-1 mediates the survival of the tumor cells.

## 3. Materials and methods

### 3.1 Tissue samples

The tissue samples were collected in collaboration with Turku University hospital from naive breast cancer patients who undergo breast ablation surgery in which the whole breast was removed. All the patients gave their consent for the use of surgical resection material in research purposes. From these tissues, pathologist provided us two types of tissue with histological confirmation: tumor tissue and adjacent “healthy” breast tissue. In addition, we also obtained blood samples from these patients. From the blood samples, the peripheral blood mononuclear cells (PBMCs) that include B-cells, T-cells, NK-cells and monocytes, were extracted. The extraction was done using density gradient centrifugation and the Ficoll-Paque® method. The tissue pieces, as well as the extracted PBMCs from the blood samples, were preserved in -150 degrees Celsius with serum containing 5% DMSO. In addition, small piece of the tissues were frozen as OCT blocks with O.C.T.<sup>tm</sup> compound (Tissue-Tek<sup>R</sup>) using moulds and dry ice for fast freeze.

## 3.2 Tumor ex vivo explant assay with stained PBMCs

### 3.2.1 PBMC treatment

Carboxyfluorescein diacetate succinimidyl ester (CFDA-SE) (Vybrant™ by Thermo Fisher Scientific) was used in staining the leukocytes to allow persistent tracking of these cells. CFDA-SE enters the cells by diffusion and is then esterized to form CFSE that bond intracellular amine residues and persists well in non-dividing cells. The dye conjugated with CFSE fluorescents at 488 $\mu$ m laser line. 5 $\mu$ M solution of CFDA-SE, diluted in PBS, was used for five million PBMCs. Incubation time for cells in CFDA-SE solution was 15 minutes in 37°C and 5% CO<sub>2</sub>. The CFDA-SE solution was removed and an additional incubation of 10 minutes with medium including serum was done to restore cell viability. Cell count was checked before and after CFSE staining. Bürker-Türk cell count chamber was used with an estimated mean count of two separate fields. Dead cells were excluded with 0.4% Trypan Blue (Thermo Fisher Scientific) staining. PBMCs were treated with anti-Cleaver-1 antibody (FP1305 from Faron Pharmaceuticals) and Human IgG4 (Ultra-LEAF™ Purified by Biolegend) antibody as a control. They were both conjugated with Alexa Fluor 640. Final concentration was 8 $\mu$ g/1x10<sup>6</sup> cells in 400 $\mu$ l of IMDM medium. One million of cells were treated with 8 $\mu$ g of either of these antibodies and an additional one million cells were used as a negative control, receiving no antibody treatment. Incubation period of 30 minutes in 37°C and 5% CO<sub>2</sub> followed.

### 3.2.2 Tumor sample coculture with PBMCs

The tumor samples were quickly heated and emptied in to 3 ml of DME medium (SIGMA Life Science) with added 10% fetal calf serum and P/S solution. Two to three pieces of the tumor sample was used. The pieces were cut in half, separating them as homogenous as possible and introducing the correlating pieces with the FP1305 or IgG4 -antibody-treated PBMCs. Also, one tissue piece of each patient was cut in three parts to get the negative control with PBMCs that were not treated with any antibodies. Tumor pieces were set in wells (Corning™ 96-Well Clear Ultra Low Attachment Microplates) containing 100 $\mu$ l IMDM medium with added 2% P/S, 2% FCS and 2% L-Glutamine. The tumors were always dense enough to stay on the bottom of the wells for the incubation period. PBMCs were introduced to the tumor tissue immediately after the 30-minute incubation. An amount of 100 $\mu$ l containing 0,25x10<sup>6</sup> of stained cells were added per well on top of the tumor samples. Incubation of 22 to 26 hours followed in 37°C and 5% CO<sub>2</sub>. After this the tissues pieces were frozen with O.C.T.<sup>tm</sup> compound (Tissue-Tek<sup>R</sup>) using moulds and dry ice for fast freeze.

### 3.3 Immunohistochemistry

For the untreated tumor and healthy assay, fixation and permeabilization was done for 6- $\mu\text{m}$ -thick tissue sections of by immersing the plates in cold acetone for five minutes. Kiovig anti-human blocking solution of 1/1000 in PBS was used to cover the plates for 20 minutes. This was done to prevent nonspecific binding of antibodies. The tissue sections were stained with an antibody solution. The solution used included following directly conjugated antibodies: Pan Cytokeratin A488 1/200 (Thermo Fisher Scientific), CD8 A555 1/100 and also FP1305 A647 10 $\mu\text{g}/\text{ml}$  antibody (Faron Pharmaceuticals) or IgG4 A647 10 $\mu\text{g}/\text{ml}$  (Ultra-LEAF™ Purified by Biolegend) as a control sample. Anti-cytokeratin was used to stain endothelial cells which, in mammary adenocarcinoma, are also the tumor cells. The staining was done in blocking solution for one hour in RT in a dark moisture chamber.

TUNEL staining method was used to stain apoptotic cells in the PBMC treated tumor tissue. Reactions were done according to the manual for tissue sections provided by the manufacturer (Click-iT™ Plus by Thermo Fisher Scientific). Kit with Alexa Fluor 594 dye was used.

Hoechst 33342 (Thermo Fisher Scientific) staining was used to detect all cells in the tissue sections. An 1/5000 solution was used with an incubation of 15 minutes in room temperature in dark. Parallel sections of the treated tumor only received Hoechst stain.

To ensure preservation, antifade reagent was added simultaneously with a coverslip. ProLong™ Gold antifade mountant (Thermo Fisher Scientific) was added and spread evenly under the coverslip. Preservation was done in 4°C in dark and imaged within a week from staining.

### 3.4 Imaging

Two types of confocal microscopes were used. The staining of untreated sections was imaged by using a Carl Zeiss LSM780 laser scanning confocal microscope. Imaged with 20x/0.8 Zeiss Plan-Apochromat objective. Three stacks with 1 $\mu\text{m}$  interval was used and a 2x2 (1952x1959 pixel) 810 $\mu\text{m}$  x 810 $\mu\text{m}$  tile area.

Imaging of the treated tissue sections was done with a spinning disk confocal microscope (by 3i). 20x magnification was used with Hamamatsu Orca Flash 4.0 detector. The imaging was done with an area of 3x3 tiles (2048 × 2048 pixel) and four 1 $\mu\text{m}$  stacks. The clearest tissue section on the plate was selected for imaging. TUNEL stained sections was imaged first and the correlating sections with only Hoechst stain was imaged after to image the correlating area of tissue if possible. Four laser lines was used on both microscopes to detect 405 $\mu\text{m}$ , 488 $\mu\text{m}$ , 561 $\mu\text{m}$  and 640 $\mu\text{m}$  channels.

### 3.5 Statistical methods

20 assays were done from immunohistochemical staining of breast adenocarcinoma tumor tissues and the adjacent healthy tissue. These samples were from randomized group of ten patients with breast ablation surgery at Turku University hospital. Assay includes 11 tumor tissue samples and 9 from adjacent healthy tissue. From the images done with confocal microscope, all CD8<sup>+</sup> cells, Clever-1<sup>+</sup> cells as well as the total amount of cells was calculated. Cells were counted from images manually using ImageJ, Version 1.52 by National Institutes of Health.

31 successful images were obtained from the tumor PBMC coculture assay. These images were analyzed with ImageJ using threshold analyzing of Hoechst stain compared to the 594 $\mu$ m channel fluorescence (TUNEL stain). The same threshold values were used for all samples.

Descriptive statistics for numerical variables are shown with means and standard deviation (sd) when assuming normal distribution and with medians and quantiles (Q1, Q3) otherwise. Confirmation of normal distribution was done with visual analysis of Q-Q-plot and using Shapiro-Wilks' test. Ordinal values are presented with frequency values and percentages. Levene test was used in evaluating equal variances of two data sets.

Significance level of 0.05 was used (two-tailed). Also, 95% confidence intervals (CI) were calculated. JMP®, Version 14.2.0 Pro. SAS Institute Inc., Cary, NC, 1989-2019

## 4. Results

### 4.1 The tissue structure and cell composition changes in mammary gland adenocarcinoma

The mammary gland is largely made up of fat and connective tissue, but its parenchyma has vasculature and a system of lobules and ducts that contribute to lactation. In breast adenocarcinoma the tumor cells originate from the epithelial cells of the duct or lobules. The difference in the localization and structure of epithelial cells can be seen in the comparison of tumor and adjacent healthy breast tissue (Figure 4). The binding of Pan Cytokeratin antibody to epithelial keratins indicates the normal duct structures in healthy tissue but on tumor tissue, these structures are disrupted. The healthy tissue samples had more fat and cells were few in the sections, whereas the tumor tissue can be seen in the images dense with a variety of cells.

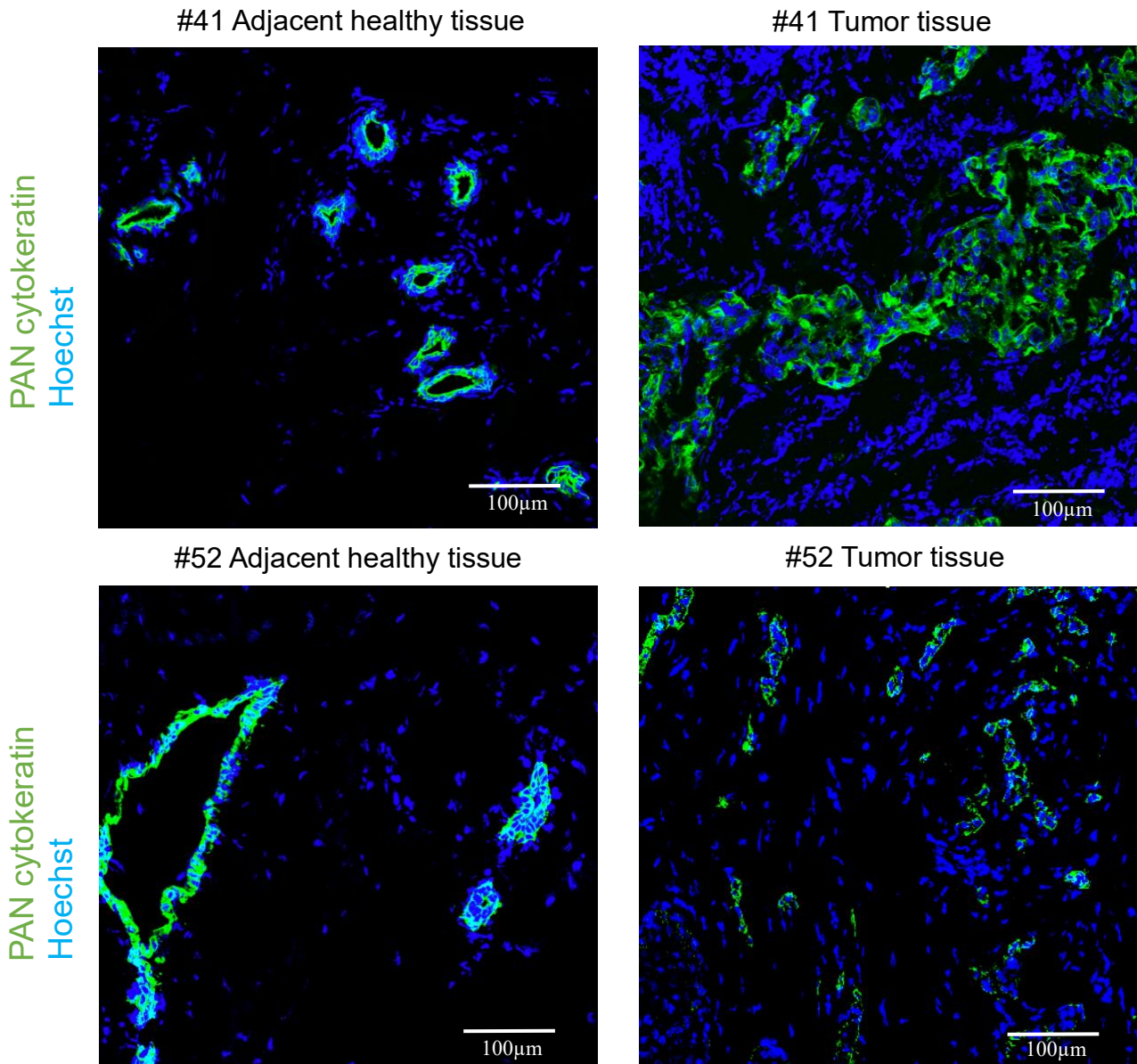


Figure 4: Comparison between immunohistochemically stained tumor sections and the adjacent healthy tissue sections from the same patient. The fluorescent colors are presented on the side.

## 4.2 Clever-1+ macrophages and CD8+ T cells are expressed in the tumor microenvironment

The representative images of tumor tissues show the presence of CD8+ T cells and macrophages expressing Clever-1 (figure 5). The images show how the TME consists of a variety of cells in addition to cancer cells. The higher density of cells on the tumor sections made it easier to show the expression of different cells than on the healthy tissues. Most of the CD8+ and Clever-1 positive cells were found from the TME surrounding the cancer cells.



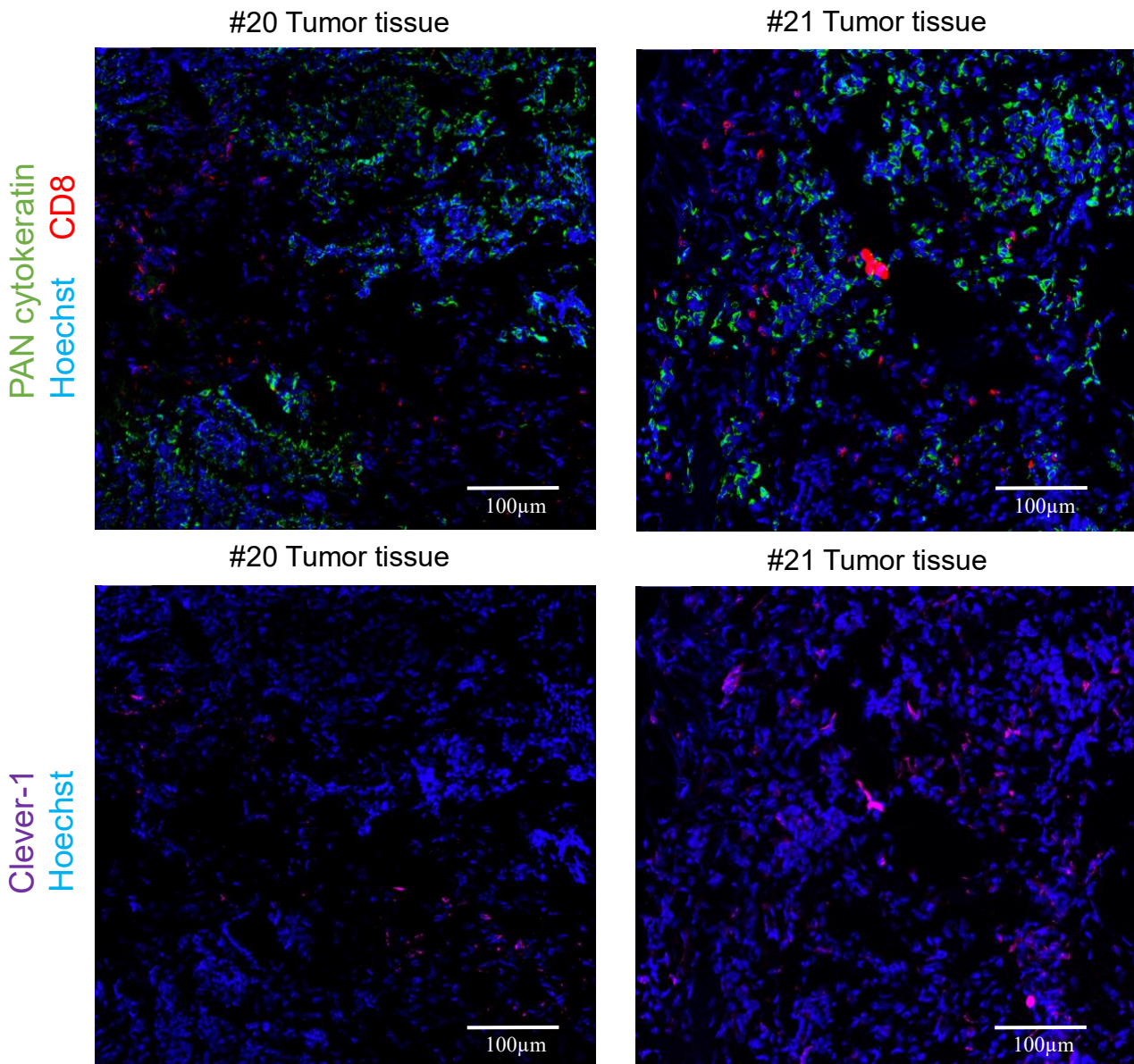


Figure 5: Clever-1 positive macrophages (magenta) and CD8+ positive T-cells (red) can be seen in correlating images of both tumor sections.

### 4.3 IHC staining cell counts

Table 1 shows the amounts of cells calculated manually from the immunohistochemically stained sections. The p-values were calculated by comparing the values from the tumor sections and the healthy tissue sections. The total amount of cells was statistically significantly higher in the tumor sections than in the adjacent healthy tissue sections ( $p=0.028$ , Wilcoxon rank sum test). Taking this into consideration, the cell number values were transformed to percentage values for more reliable analysis. The percentage values of CD8+ T cells and Clever-1+ macrophages did not prove statistically significant in the comparison of tumor and the adjacent healthy tissue. A correlation graph (figure 6), shows the amounts of T cells and macrophages in the tissue sections.

Table 1: The sum amounts of cells in tumor and adjacent healthy tissue counted manually with the ImajeJ program.

|  | Total, n= 20      | Tumor tissue, n= 11 | Healthy tissue, n=9 | p-value |
|--|-------------------|---------------------|---------------------|---------|
| Total cells, Median (Q1, Q3)                       | 384 (276, 613)    | 514 (342, 730)      | 302 (142, 392)      | =0.028* |
| CD8+ cells, Median (Q1, Q3)                        | 83.8 (64, 130)    | 110 (76, 168)       | 65 (27, 84)         | =0.033* |
| Percentage (%) of CD8+ cells, Median (Q1, Q3)      | 16.4 (12.5, 31.2) | 15.1 (12.0, 35.4)   | 17.4 (12.9, 31.0)   | =0.93*  |
| Clever-1+ cells, Median (Q1, Q3)                   | 15 (6, 46)        | 9 (5, 83,5)         | 18 (7, 42)          | =0.62*  |
| Percentage (%) of Clever-1+ cells, Median (Q1, Q3) | 5.5 (1.4, 8.3)    | 2.3 (1.0,8.1)       | 6.5 (4.9, 18.2)     | =0.15*  |

\* Wilcoxon rank sum-test

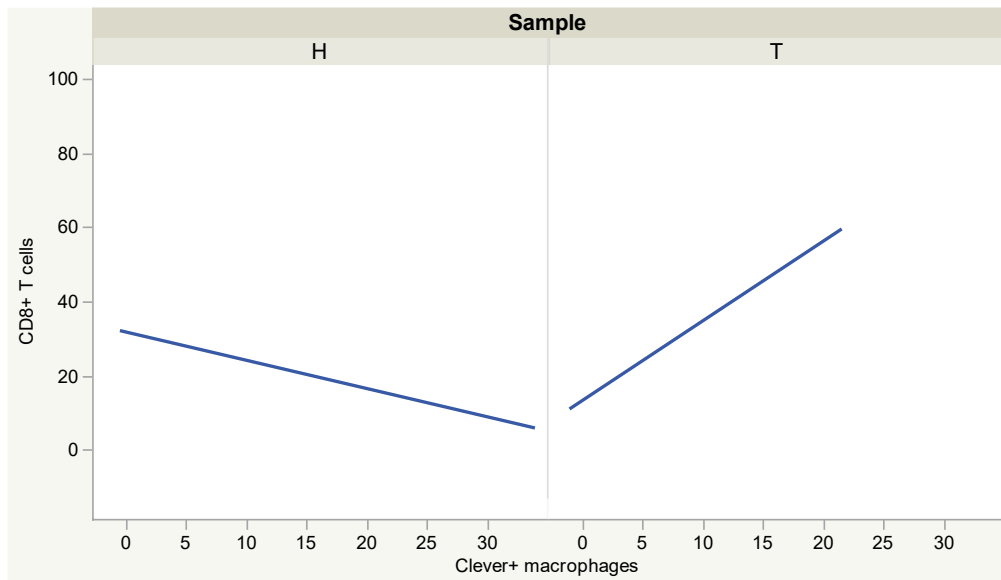


Figure 6: Correlation graph with fitted linear regression with confidence intervals (0.95) of Clever-1+ macrophages in relation to the amount of CD8+ T cells. H is for the adjacent healthy tissue and T stands for tumor.

#### 4.4 Treated PBMCs migrate into the tumor tissue

CFSE labeled PBMC cells were often seen on the sections on the outer line of the section on the edge of the tumor tissue. But as seen in an image of tumor section from patient #38 in figure 7, CFSE+ cells can be seen clearly also in the middle of the sections that were from two to five mm wide.

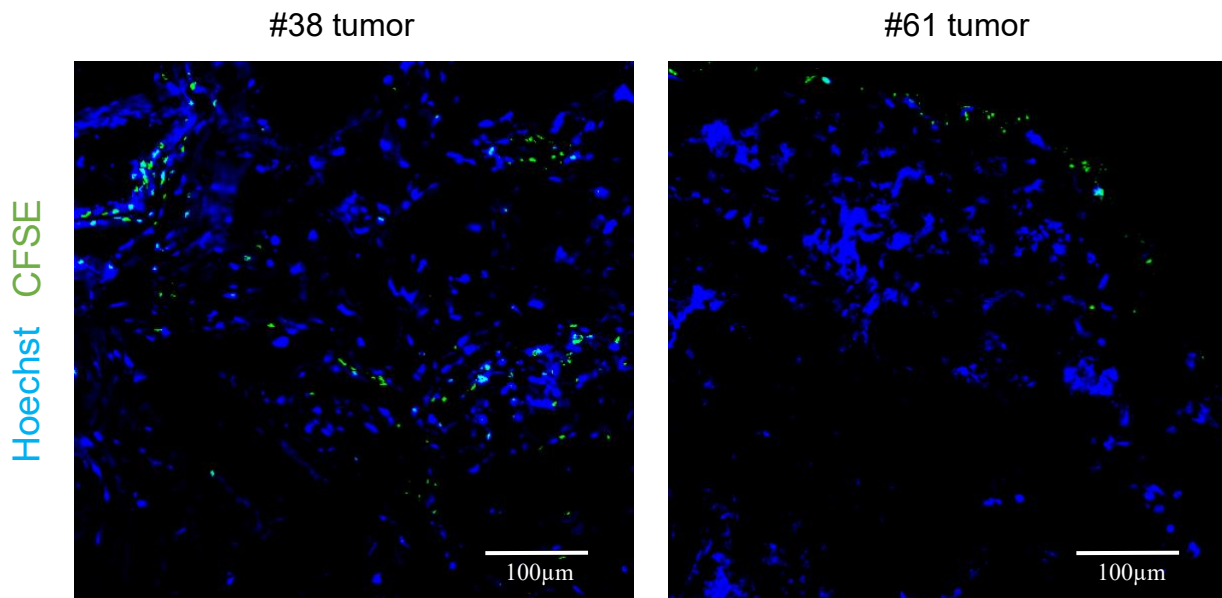


Figure 7: CFSE labeled PBMC cells are seen in sections of tumors when cocultured together.

#### 4.5 Anti-Clever-1 antibody treated leukocytes induce apoptosis in tumor cells

The TUNEL apoptosis detection kit showed some non-specific fluorescence in the tissue sections but the apoptotic cells could be clearly differentiated as pink, where the TUNEL stained double positive with the Hoechst stain (figure 8). Anti-Clever-1 treated PBMCs induced apoptosis significantly in the tumor tissue in comparison to the controls.

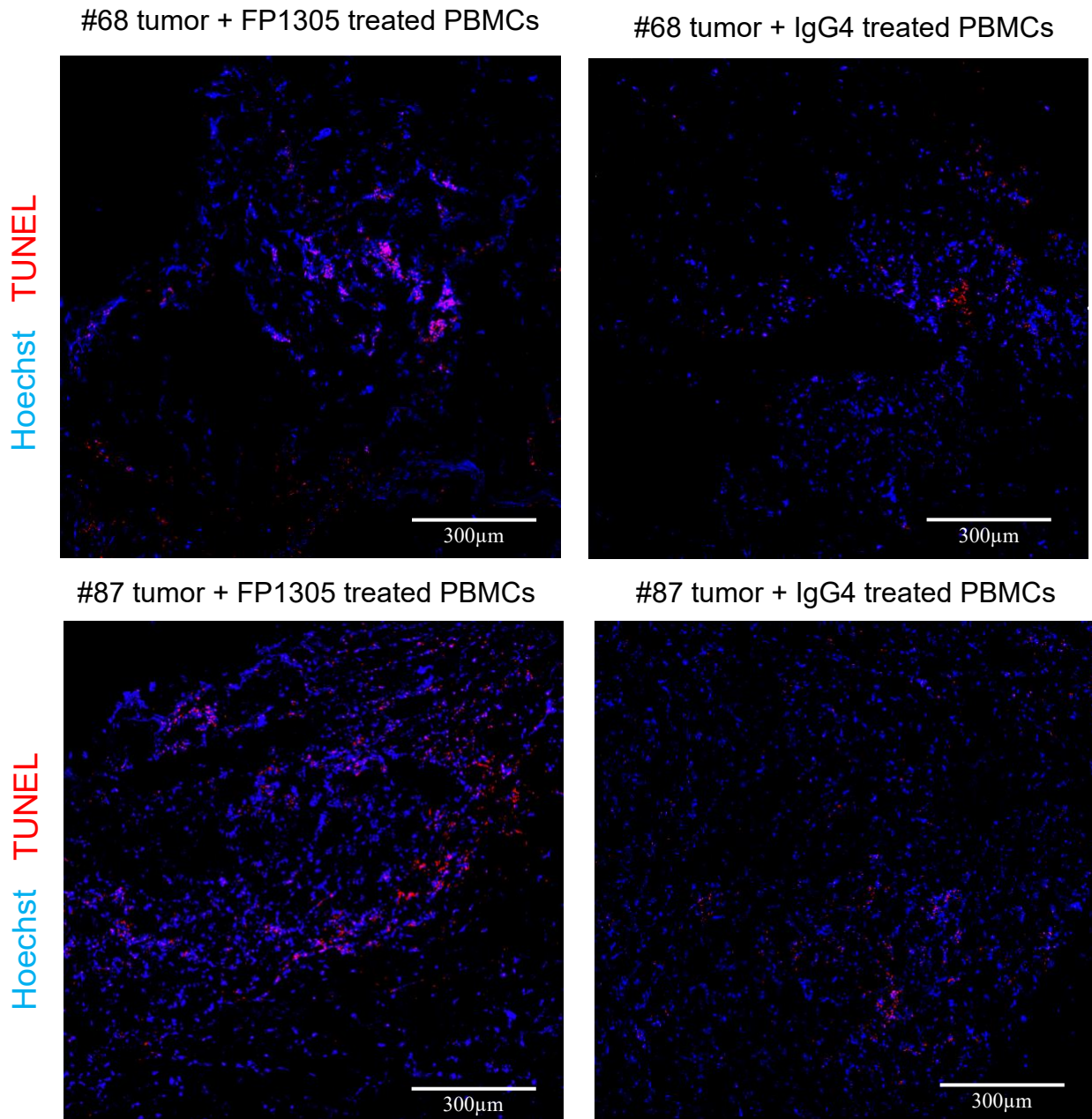


Figure 8: Positive TUNEL binding seen in apoptotic cells in comparison of two patient samples with correlative IgG4 control

Table 2 summarizes the values from the threshold analysis done on the tumors stained with the TUNEL apoptosis detection kit. 31 microscope images were analyzed overall, including 12 with FP1305, 12 with IgG4 control, four of untreated PBMC controls and finally an additional three images of control tumors not treated with PBMCs. Average of the results from each patient assay was used in analyzes. The presented p-values were calculated by comparing the values in the anti-Clever-1 -treated PBMC assay with the results from the IgG4-antibody-control assay.

Table 2: Values from image analysis of treated tumors

|                              | Total n= 10    | Anti-Clever-1-treated PBMCs, n=5 | IgG4-antibody control, n=5 | Untreated PBMC ctrl, n=4 | Tumor negative ctrl, n=3 | p-value              |
|------------------------------|----------------|----------------------------------|----------------------------|--------------------------|--------------------------|----------------------|
| Total cell value, mean (sd)  | 107458 (53419) | 136292 (38579)                   | 118689 (66819)             | 64420 (55680)            | 98069 (6421)             | =0.1107 <sup>^</sup> |
| TUNEL stain value, mean (sd) | 17847 (11668)  | 27946 (8367)                     | 17527 (9202)               | 5623 (3784)              | 13201 (3931)             | =0.0983 <sup>^</sup> |
| CFSE+ PBMCs, mean (sd)       | 27,7 (18,4)    | 39.9 (21,2)                      | 27,1 (13,3)                | 13,3 (10,2)              | 1,33 (1,15)              | =0.8268 <sup>^</sup> |

<sup>^</sup> two-sample t-test assuming unequal variances

The three controls of the untreated tumors showed a minimal amount of false positive results on the amount of CFSE+ cells with a mean (sd) value of 1.33 (1.15), which was statistically significantly different ( $p=0.0003$ , two-sample t-test assuming unequal variances). These false positives result from autofluorescence of the adjacent tissue structures on the 488 $\mu$ m channel.

Results from the TUNEL positive staining on tumor sections between the anti-Clever-1 treated PBMC assay and the IgG4 control did not reach statistical significance ( $p=0.0983$ , two-sample t-test assuming unequal variances). However, with visual examination of the TUNEL sections, it is clear that statistical significance would be achieved in a study with a larger n. The variance in the amount of apoptosis in the sections can be visually seen from the microscope images in figure 8.

The amount of migrated CFSE+ cells in the anti-Clever-1 tumor sections did not prove statistically significant ( $p=0.8268$ , two-sample t-test assuming unequal variances). In this analysis the amount of CFSE+ cells were standardized to the total amount of cells. But yet, the sections with highest amount of migrated CFSE+ cells were seen on the anti-Clever-1 assays with mean (sd) value of 39.9 (18.4). What is more, figure 9 indicates a higher amount of apoptosis in sections with more migrated CFSE+ PBMCs seen.

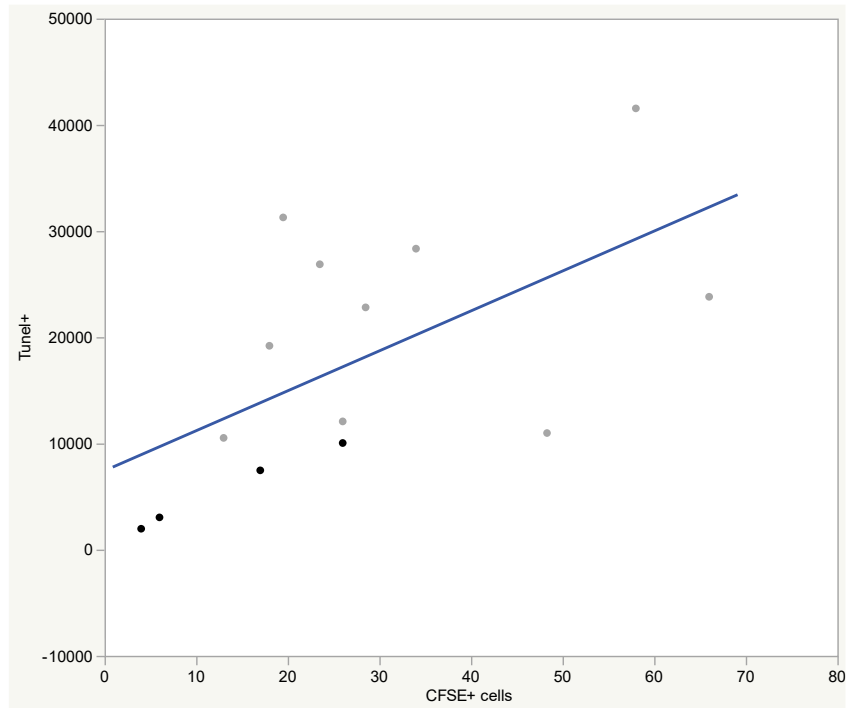


Figure 9: Correlation graph of fitted linear regression with 95% confidence intervals. All the data in table 2 was used except from the negative controls without PBMC coculture.

## 5. Discussion

The research of cancer immunology has shown significant results in introducing modern approaches in treating various cancer types with unprecedented results. In clinical use, activating the antitumor response of the immune system has resulted in excellent responses with gross reduction of tumor growth and metastasis. Re-establishing inflammation in the tumor with the use of ICB therapies, gives access for new and old cancer therapies to be used in combination. In this study, the involvement and function of the innate immune system, in this case the macrophages in cancer, is studied in detail. The donated tissue material from breast cancer patients provided a good opportunity to mimic tissue behavior much more precisely compared to the use of 2D cell cultures and to study the composition of the tumor tissue in detail and also to monitor tumor response *ex vivo*.

The Alexa 647 conjugated anti-Clever-1 antibody proved very specific in binding Clever-1 in the tissue. This enabled us to examine immunohistochemically the localization of the Clever-1+ macrophages in the tumor microenvironment. The objective in the first part of this study was to elucidate the amount of expression of Clever-1+ cells in relation to other cells present in the TME. Since all the material was from breast adenocarcinoma, we show that Pan Cytokeratin staining together with abnormal structure offers a sufficient tumor cell marker in tumor sections. CD8 staining proved a specific T cell marker in the sections. All the treatments were done on previously untreated and unfixed tissue sections so that we could image the *in vivo* cell composition of the tissues. Our hypothesis was based on previous studies with Clever-1, that the expression of Clever-1+ macrophages is increased in the tumor site. Our results with immunohistochemically stained tumor sections did show high expression of Clever-1+ macrophages. Surprisingly CD8+ cells were also highly expressed in tissues with Clever-1+ macrophages, even though the Clever-1+ macrophages should in theory reduce the amount of anti-tumor immune cells like CD8+ T cells in the TME. While the CD8 antibody works well as a specific T cell marker, it does not on the other hand show the functionality of the T cells. Hence, it is not known whether they are the actual cytotoxic anti-tumor phenotype. This requires further studies with comparison of the amounts of activated CTLs, with the use of antibody detection of the PD-1 receptor or granzyme B measurement (28), to the amount of overall CD8+ T cells in the TME.

An interesting result was shown in comparing the cell composition of the tumor tissue with the cells in the adjacent healthy tissues. It was shown that in the adjacent healthy tissue, the amount of Clever-1+ macrophages seemed to correlate with lower counts of CD8+ T cells. This was in contradiction to the result seen in the actual tumor sections. Still, no definitive conclusions can be made, and further studies should follow for example with assays using flow cytometry, where the cell composition in tissues can

be analyzed quantitatively. The healthy tissues proved less dense with cell material and this could falsify the results in this assay.

The *ex vivo* assay done on the tumor tissue samples was the main method of this study. The main purpose was to image the biological effect of the anti-Clever-1 antibody treatment. PBMCs, cells that play a major role in tumor depletion, circulate in the blood and their migration to the tumor site is an essential factor in cancer prognosis. As the monocytes migrate into tissue, they differentiate into macrophages of distinct subtypes as reviewed in chapter 2.3. Treating these monocytes with anti-Clever-1, is supposed to (11) affect the differentiation so that the anti-inflammatory M2 subtype proliferation is decreased and the anti-tumor and pro-inflammatory subtype M1 will dominate. The M1-type migration to the tumor site should increase the anti-tumor activation of cytotoxic T cells and apoptosis of tumor cells. This effect of anti-Clever-1 treatment was studied in a way that the anti-Clever-1 antibody was separately introduced to the PBMCs before coculturing them with the tumors. The PBMCs used in the assay originated from the same patients as was the treated tumor tissue to accurately mimic *in vivo* conditions. Controls of this method was done in diverse ways, with the use of IgG4 antibody instead of anti-Clever-1 antibody and in addition with untreated PBMCs. Also, some negative controls were done with tumors cocultured without any PBMCs. The results from analyzing the fluorescent area of the DNA stain (Hoechst) in comparison to the apoptosis stain (TUNEL) gave the result on the amount of apoptosis present in the tumors in the time of freezing after the 24-hour-coculture with PBMCs. When visually examining the sections with confocal microscope, the results were distinct. In the tumors cocultured with anti-Clever-1 treated PBMCs, a constant degree of apoptosis was seen on the large tumor cells in pink clusters where the DNA stain and TUNEL stained double positive. What is more, as the sections were cut with cryostat, a consistent cut of 100 $\mu$ m was done on the tumor surface until the actual sections were cut. This proves that the apoptosis was not only induced in the tumor cells close to the surface but also deep in the tumor tissue. The IgG4 -antibody control showed an increased rate of apoptosis compared to the other controls done, but still the difference in the anti-Clever-1-treated tissue was visible. The image analysis used is not accurate in getting definite numbers, but done with linear settings for all the samples, it was adequate in getting a significant difference on the amount of apoptosis present in the tumors. As the study cohort is small, any large-scale statistical analysis must be done with caution. With more collateral experiments done on the same patients' tumor tissue samples, the assay would arguably provide statistically significant results with a larger sample quantity.



PBMCs cocultured with the tumor were able to be seen in the tumor sections due to CFSE staining done prior to the coculture. Penetration of these CFSE<sup>+</sup> cells were seen in all samples (except the negative controls with no PBMCs introduced) deep in the middle of the tumor tissue. No significant permeabilization ability was proven in the PBMCs treated with the anti-Cleaver-1 antibody. This was not the main question to be answered though, since it is known that macrophages secrete cytokines that, in turn, increase the cytotoxic functions of the CTLs for example. To have effect on the tumor apoptosis, the anti-Cleaver-1 macrophages do not necessarily require close contact with the tumor cells.

The problem with the 594 $\mu$ m dye, that was used in the TUNEL kit, is that the fluorescence reaches both 561 $\mu$ m and 640 $\mu$ m laser channel. This meant that we were not able to differentiate Cleaver-1<sup>+</sup> cells on the 640 $\mu$ m channel from the apoptotic cells. We were not able to get results on how the Cleaver-1<sup>+</sup> cells localized in relation to apoptotic tumor cells, but yet Cleaver-1<sup>+</sup> cells were consistently seen in the secondary sections done with just the DNA stain. No CFSE<sup>+</sup> cells with double positive Cleaver-1 stain was seen on the sections, but this could be due to the CFSE stain not persisting on the macrophages after differentiation from the blood monocytes.

In conclusion, utilizing the unique patient material acquired from Turku University hospital we were able to study the cell compositions in detail in both healthy and tumor tissue in breast adenocarcinoma. CD8<sup>+</sup> T cells and Cleaver-1<sup>+</sup> macrophages were consistently seen in both the tumor TME as well as in the adjacent healthy tissue. Further studies are needed to define the cytotoxic activation of the T cells in the TME. Cleaver-1<sup>+</sup> macrophages were commonly seen in the tissue sections which is in-line with previous studies. This study provided essential information on the localization of these Cleaver-1<sup>+</sup> macrophages in relation to CD8<sup>+</sup> T cells and cancer cells, in the TME. In addition, we conducted a novel assay with the treatment of patient derived PBMCs with the anti-Cleaver-1 antibody and coculturing these cells with the corresponding patient tumor tissue explants. The results clearly show how these anti-Cleaver-1 treated PBMCs induce higher amounts of apoptosis in the tumor compared to the controls. This assay thus proved unprecedented results on anti-Cleaver-1 treatment's biological effects in the tumor site and is a solid addition to previous studies on the subject. What is more, this novel explant assay is applicable to be used in further studies using different combinations of antibodies and in imaging their biological effects in the tissue, *ex vivo*.

## 6. References

1. Bray F, Ferlay J, Soerjomataram I et al. Global cancer statistics 2018: GLOBOCAN estimates of incidence and mortality worldwide for 36 cancers in 185 countries. *CA Cancer J Clin* 2018;68(6):394-424
2. Teng MW, Galon J, Fridman WH, Smyth MJ. From mice to humans: developments in cancer immunoediting. *J Clin Invest* 2015; 125(9):3338-46
3. Howe LR, Subbaramaiah K, Hudis CA, Dannenberg AJ. Molecular pathways: adipose inflammation as a mediator of obesity-associated cancer. *Clin Cancer Res* 2013; 19(22):6074-83
4. Askeland EJ, Newton MR, O'Donnell MA, Luo Y. Bladder Cancer immunotherapy: BCG and Beyond. *Adv Urol* 2012; 2012:181987
5. Slamon DJ, Clark, GM et al. Human breast cancer: correlation of relapse and survival with amplification of the HER-2/neu oncogene. *Science* 1987; 235(4785): 177-82
6. Rodig S, Guseleitner D et al. MHC proteins confer differential sensitivity to CTLA-4 and PD-1 blockade in untreated metastatic melanoma. *Science Translational Medicine* 2018; 10(450): 3342
7. Brand A, Singer K, Koehl GE et al. LDHA-associated lactic acid production blunts tumor immunosurveillance by T and NK cells. *Cell Metab.* 2016; 24(5): 657–671
8. Ouyang W et al. Regulation and functions of the IL10 family of cytokines in inflammation and disease. *Annu. Rev. Immunol.* 2011; 29: 71-109
9. Travis MA, Sheppard D. TGF $\beta$  activation and function in immunity. *Annu. Rev. Immunol.* 2014; 32: 51-82
10. Sharma P, Allison JP. Immune checkpoint targeting in cancer therapy: toward combination strategies with curative potential. *Cell* 2015; 161(2): 205-14
11. Viitala M, Virtakoivu R, Tadayon S et al. Immunotherapeutic Blockade of Macrophage Clever-1 Reactivates the CD8<sup>+</sup> T-cell Response against Immunosuppressive Tumors. *Clin Cancer Res* 2019; 25(11): 3289-3303
12. Iannello A, Thompson TW, Ardolino M, Marcus A, Raulet DH. Immunosurveillance and immunotherapy of tumors by innate immune cells. *Curr Opin Immunolol.* 2016; 38: 52-8
13. Coffelt SB, Kersten K, Doornebal CW et al. IL-17-producing  $\gamma\delta$  T cells and neutrophils conspire to promote breast cancer metastasis. *Nature* 2015; 522(7556): 345-348

14. Varricchi G, Loffredo S, Galdiero MR et al. Innate effector cells in angiogenesis and lymphangiogenesis. *Curr Opin Immunol* 2018; 53: 152-160
15. Donskov F. Immunomonitoring and prognostic relevance of neutrophils in clinical trials. *Semin Cancer Biol* 2013; 23(3): 200-7
16. Mosser DM, Edwards JP. Exploring the full spectrum of macrophage activation. *Nat Rev Immunol.* 2008; 8(12): 958-69
17. Zhang QW et al. Prognostic significance of tumor-associated macrophages in solid tumor: a meta-analysis of the literature. *PLoS one* 2012; 7(12): e50946
18. Murakami Y et al. Increased regulatory B cells are involved in immune evasion in patients with gastric cancer. *Sci Rep* 2019; 9(1) 13083
19. Matsushita H et al. Cancer exome analysis reveals a T-cell-dependent mechanism of cancer immunoediting. 2012; 482(7385): 400-4
20. Davis MM, Bjorkman PJ. T-cell antigen receptor genes and T cell recognition. *Nature* 1988; 334(6181): 395-402
21. Robert C, Thomas L, Bondarenko I et al. Ipilimumab plus dacarbazine for previously untreated metastatic melanoma. *N Engl J Med* 2011; 364(26): 2517-26
22. Hodi FS, O'Day SJ, McDermott DF et al. Improved survival with ipilimumab in patients with metastatic melanoma. *N Engl J Med* 2010; 363(8): 711-23
23. Michot JM, Bigenwald C, Champiat S. Immune-related adverse events with immune checkpoint blockade: a comprehensive review. *Eur J Cancer* 2016; 54: 139-148
24. Mantovani A, Marschesi F, Malesci A et al. Tumour-associated macrophages as treatment targets in oncology. *Nat. Rev. Clin. Oncol.* 2017; 14(7): 399-416
25. Kzhyshkowska J, Gratchev A, Goerdts S. Stabilin-1, a homeostatic scavenger receptor with multiple functions. *J. Cell. Mol. Med.* 2006; 10(3): 635-49
26. Palani S, Elima K, Ekholm E. Monocyte Stabilin-1 Suppresses the Activation of Th1 Lymphocytes. *J. Immunol.* 2016; 196(1): 115-23
27. Karikoski M, Marttila-Ichihara F, Elima K et al. Clever-1/stabilin-1 controls cancer growth and metastasis. *Clin. Cancer Res.* 2014; 20(24): 6452-64
28. Zvan A, Bi K, Norwitz ER et al. Mixed signature of activation and dysfunction allows human decidual CD8+ T cells to provide both tolerance and immunity. *Proc. Natl. Acad. Sci. USA* 2018; 115(2): 385-390